

Mapping the phase diagram of spinor condensates via adiabatic quantum phase transitions

J. Jiang, L. Zhao, M. Webb, and Y. Liu*

Department of Physics, Oklahoma State University, Stillwater, OK 74078

(Dated: April 29, 2014)

We experimentally study two quantum phase transitions in a sodium spinor condensate immersed in a microwave dressing field. We also demonstrate that many previously unexplored regions in the phase diagram of spinor condensates can be investigated by adiabatically tuning the microwave field across one of the two quantum phase transitions. This method overcomes two major experimental challenges associated with some widely used methods, and is applicable to other atomic species. Agreements between our data and the mean-field theory for spinor Bose gases are also discussed.

PACS numbers: 67.85.Hj, 03.75.Mn, 67.85.Fg, 03.75.Kk

A spinor Bose-Einstein condensate (BEC) is a multi-component BEC with an additional spin degree of freedom, which has provided exciting opportunities to study quantum magnetism, superfluidity, strong correlations, spin-squeezing, and massive entanglement [1–5]. The interesting interactions in spinor BECs are interconversions among multiple spin states and magnetic field interactions (or microwave dressing field interactions) characterized by q_{net} , the net quadratic Zeeman energy. The interplay of these interactions leads to oscillations among multiple spin populations, which has been experimentally confirmed in $F=1$ ^{23}Na spinor BECs [6–12], and in both $F=1$ and $F=2$ ^{87}Rb spinor condensates [13–17].

Several groups demonstrated the mean-field (MF) ground states of spinor BECs by holding BECs in a fixed magnetic field and letting spin population oscillations damp out over a few seconds [8–11]. The required damping time, determined by energy dissipation, may in some cases exceed the BEC lifetime. The exact mechanism involved in energy dissipation requires further study, although it has been shown that energy dissipates much faster in high magnetic fields [10]. For $F=1$ BECs, a magnetic field introduces only a positive q_{net} , while a microwave field has a distinct advantage since it can induce both positive and negative q_{net} [1, 7, 12, 18, 19]. As shown in Ref. [12], the same physics model explains spin-mixing dynamics observed in both microwave fields and magnetic fields. One would assume that, if given a long enough exposure to a microwave field, a spinor BEC could also reach its MF ground states. However, experimental studies on ground states of spinor BECs in microwave fields have proven to be very difficult, since these fields are created by near-resonant microwave pulses. Two major experimental challenges associated with microwave fields are atom losses and variations in magnetization m . Microwave-induced changes in both m and the atom number N can be detrimental, especially when a spinor BEC is exposed to a large microwave field for a prolonged time [7, 12]. As a result, the phase diagram of $F=1$ BECs has not been well explored in the $q_{\text{net}} \leq 0$ region, where applying microwave fields may be necessary.

In this paper, we demonstrate a new method to overcome the aforementioned experimental challenges and report the observation of two quantum phase transitions in a spinor BEC. In this method, we quickly prepare an initial equilibrium state at a very high magnetic field to minimize the damping time for spin population oscillations and prevent unnecessary exposure to microwave pulses. Equilibrium states at a desired q_{net} are then created by adiabatically sweeping an additional microwave field. Using this method, we are able to investigate many previously unexplored regions in the phase diagram of antiferromagnetic spinor BECs and observe three distinct quantum phases. Similarly to Ref. [1, 2, 11], we define three phases in the MF ground states based on ρ_0 , the fractional population of the $|F=1, m_F=0\rangle$ state: $\rho_0 = 1$, $\rho_0 = 0$, and $0 < \rho_0 < 1$ respectively represent a longitudinal polar phase, an antiferromagnetic (AFM) phase, and a broken-axisymmetry (BA) phase. We observe two quantum phase transitions: one is between a longitudinal polar phase and a BA phase at a fixed positive q_{net} , and the other is an AFM-BA phase transition at a given m . We also calculate the energy gap between the ground states and the first excited states in a spinor BEC, which provides an explanation for the feasibility of this new method. In addition, spin domains and spatial modes are not observed in our system, and our data can be well fit by predictions of the single spatial-mode approximation (SMA).

The SMA assumes all spin states share the same spatial wavefunction, which has been a successful model to understand spinor microcondensates [8–13, 20–22]. After taking into account that N and m are independent of time t and neglecting all constant terms in the Hamiltonian of spinor BECs, we use the SMA to express the BEC energy E and the time evolution of ρ_0 and θ as [1, 20, 21]

$$E(t) = c\rho_0(t)\{[1 - \rho_0(t)] + \sqrt{[1 - \rho_0(t)]^2 - m^2} \cos[\theta(t)]\} + q_{\text{net}}(t)[1 - \rho_0(t)] ; \quad (1)$$

$$\dot{\rho}_0 = -\frac{4\pi}{h} \frac{\partial E(t)}{\partial \theta(t)}, \quad \dot{\theta} = \frac{4\pi}{h} \frac{\partial E(t)}{\partial \rho_0(t)}. \quad (2)$$

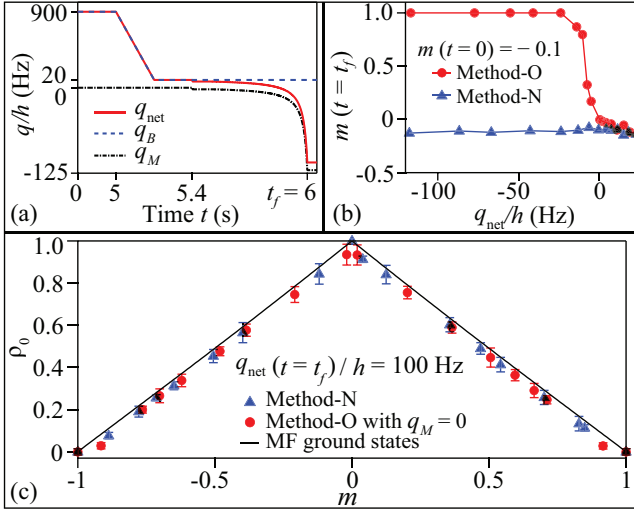


FIG. 1. (color online) (a). A typical experimental sequence of Method-N, which is our new method to create equilibrium states via adiabatically sweeping a microwave field. In this paper $-150 \text{ Hz} \leq q_{\text{net}}(t = t_f)/h \leq 150 \text{ Hz}$. All axes are not to scale. (b). m as a function of q_{net} at $t = t_f$ in the two methods starting from the same initial state, i.e., $m(t = 0) = -0.1$. Note that t_f for Method-O in this panel is only 1 s, which is much shorter than the typical hold time for creating equilibrium states. (c). ρ_0 as a function of m at $q_{\text{net}}(t = t_f)/h = 100 \text{ Hz}$ in equilibrium states created by the two methods. In this panel, Method-O prepares equilibrium states by holding BECs for 8 s in a high magnetic field where $q_M = 0$ and $q_B/h = 100 \text{ Hz}$. The solid black line represents the MF ground states (see text).

Here $q_{\text{net}} = q_M + q_B$ is the net quadratic Zeeman energy with q_B (or q_M) being induced by magnetic (or microwave dressing) fields. The spin-dependent interaction energy c is proportional to the atom density, and is positive (or negative) in $F=1$ antiferromagnetic ^{23}Na (or ferromagnetic ^{87}Rb) spinor BECs. For example, c/h is 40 Hz for our ^{23}Na system in this paper, where h is the Planck constant. The fractional population ρ_{m_F} and the phase θ_{m_F} of each m_F state are independent of position in SMA, and $m = \rho_{+1} - \rho_{-1}$. The relative phase among the three m_F spin states is $\theta = \theta_{+1} + \theta_{-1} - 2\theta_0$.

By minimizing Eq. (1), we find ρ_0 in a MF ground state of $F=1$ spinor BECs is zero if $q_{\text{net}} < c(1 \pm \sqrt{1 - m^2})$; or equals to one if $m = 0$ and $q_{\text{net}} > -c(1 \pm 1)$; or is the root of the following equation at all other q_{net} and m ,

$$c[1 - 2\rho_0 \pm \frac{(1 - 2\rho_0)(1 - \rho_0) - m^2}{\sqrt{(1 - \rho_0)^2 - m^2}}] - q_{\text{net}} = 0, \quad (3)$$

where the $+$ (or $-$) sign applies to ferromagnetic (or antiferromagnetic) spinor BECs. Typical MF ground states of spin-1 sodium BECs are shown in Figs. 1 and 2. Our experimental phase diagram and the theoretical phase diagram based on Eq. (1-3) are also plotted in Fig. 3.

The experimental setup is similar to that elaborated

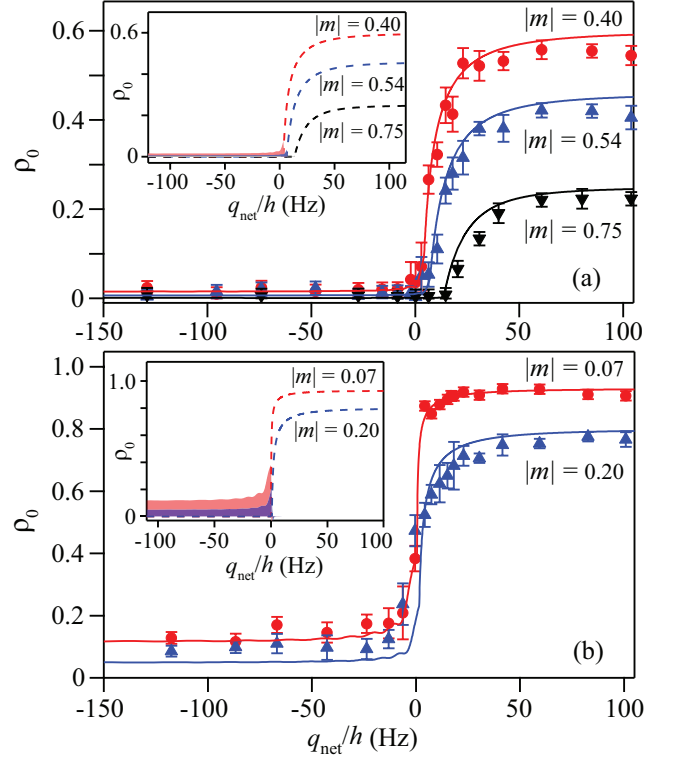


FIG. 2. (color online) ρ_0 as a function of q_{net} at $t = t_f$ for three large $|m|$ in Panel (a) and for two small $|m|$ in Panel (b) in equilibrium states created by our new method. Solid lines are simulation results for the experimental processes based on Eq. 2 (see text). Insets: dashed lines are the MF ground states. Shaded areas represent the differences between our simulation results and the MF theory at various m . The black, blue, and red colors in Panel (a) respectively correspond to results at $|m| = 0.75, 0.54$, and 0.40 . The blue and red colors in Panel (b) represent results at $|m| = 0.20$ and 0.07 , respectively.

in our recent publications [6, 12]. A $F=1$ BEC of 5×10^4 atoms is created by a forced evaporation in a crossed optical dipole trap. To fully polarize atoms into the $|F = 1, m_F = -1\rangle$ state, we turn on a weak magnetic field gradient and a low magnetic bias field in the forced evaporative cooling process. A resonant rf-pulse of a proper amplitude and duration is applied to prepare an initial state with any desired combination of the three m_F states. This moment is defined as the starting point ($t = 0$) of our experimental sequences, as shown in Fig. 1(a). Every sequence ends at $t = t_f$. Populations of multiple spin states are then measured by a standard Stern-Gerlach absorption imaging.

We use two different methods to generate equilibrium states. The Method-O is an old and widely-used method, which creates equilibrium states simply by holding a BEC at a fixed q_{net} for a sufficiently long time. We find that the required hold time is longer than 2 s for all positive q_{net} studied in this paper. This old method fails for

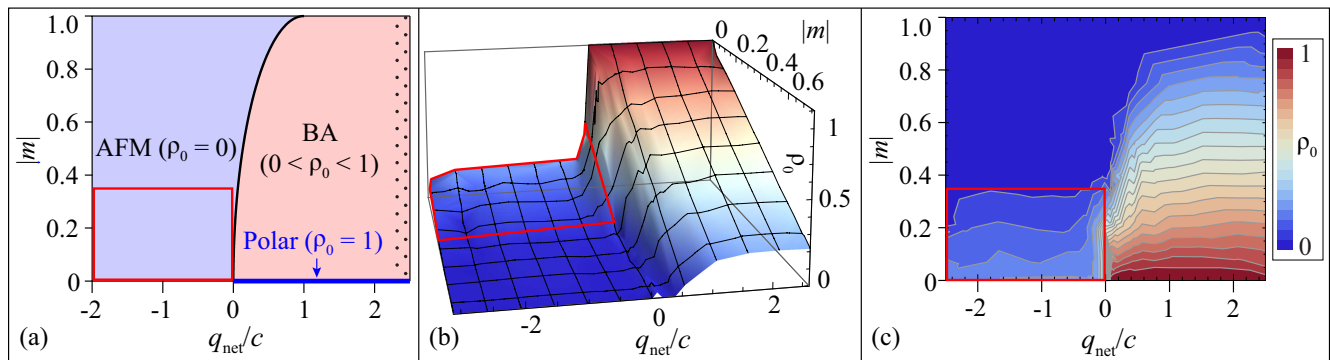


FIG. 3. (color online) (a). The MF phase diagram of spin-1 antiferromagnetic spinor BECs based on Eqs. (1-3). Our new method works everywhere except in the area marked by red solid lines, while Method-O only applies to the area filled with dots at large q_{net} . Panel (b) (or (c)) is a 3D (or a contour) plot of the experimental phase diagram consisting of data taken by our new method at 153 different q_{net} and m . Red solid lines in Panels (b)-(c) mark the region where our data are different from the MF ground states.

our system in low magnetic fields (i.e, the small positive q_{net} region), because energy dissipates very slowly and the required hold time is longer than the BEC lifetime (~ 10 s) in this region. This old method is more problematic in the negative q_{net} region, because it leads to significant atom losses and detrimental changes in m . In order to overcome these experimental challenges associated with the old method, we have developed a new method, Method-N. A comparison of these two methods starting from the same initial state is shown in Fig. 1(b), which highlights the advantage of our new method. A typical experimental sequence of the new method is listed in Fig. 1(a). We first hold a spinor BEC in the optical trap for 5 s at a very high magnetic field with $q_B/h = 900$ Hz. This step ensures the BEC reaches its ground states, since we and Ref. [10] find that the energy dissipation rate quickly increases with q_B . Second, we adiabatically ramp the magnetic field down to $q_B/h = 20$ Hz in 0.1 s, keep q_B at this value for 0.3 s, and then turn on a far off-resonant microwave pulse in 0.1 s. Third, we tune only the frequency of this pulse slowly within 0.5 s, in order to adiabatically sweep its corresponding microwave field to a desired q_{net} . Our approach to characterize microwave dressing fields and the frequency tuning curve for adiabatically sweeping q_{net} within the range of $-\infty$ to $+\infty$ are as same as those illustrated in our previous work [12].

In theory, once a BEC is prepared into its ground state, the BEC may stay in its ground state at each q_{net} when a microwave field is adiabatically ramped [3]. We can thus initially check whether the new method is applicable by comparing equilibrium states created by both new and old methods in a region, $q_{\text{net}} \gg 0$, where the old method has been proven to generate the MF ground states [8–11]. Figure 1(c) shows such comparisons made at $q_{\text{net}}(t = t_f)/h = 100$ Hz for various magnetization m . The equilibrium states created by the two methods appear to be quite similar, and they stay very close to the

same black solid line which represents the MF ground states in Fig. 1(c). This suggests that our new method is adiabatic enough to replace the old method in studies related to the BEC phase diagrams. We also find that a spinor BEC returns to its original state when we ramp a microwave field from $q_M = 0$ to a fixed nonzero q_M and then back to $q_M = 0$ with this new method, although this observation may not be sufficient to prove the process is adiabatic.

We then apply our new method to a much wider range of q_{net} and m , especially in the negative and small positive q_{net} regions which cannot be easily explored by the old method, as shown in Fig. 2. We find two interesting results from this figure. First, our data in Fig. 2(a) show a quantum phase transition between a BA phase and an AFM phase at each m . This BA-AFM phase transition appears to occur at a larger q_{net} when $|m|$ gets bigger, which can be well explained by the MF theory (i.e., dashed lines in the inset in Fig. 2(a)). Another interesting result is that this new method does allow us to access many previously unexplored regions in the phase diagram, although there is a visible discrepancy between the MF ground states and our data at a small m in the negative q_{net} region, as shown in Fig. 2(b). To understand this phenomenon, we simulate the experimental processes based on Eq. 2 by taking a proper formula to account for the time evolution of q_{net} during an adiabatic ramping of microwave fields. Figure 2 shows that the simulation results can well resemble the experimental data, while the differences between our simulation results and the MF ground states are emphasized by a shaded area at each m in the two insets in Fig. 2. These shaded areas appear to slowly increase in the negative q_{net} region when $|m|$ approaches zero. In other words, the discrepancy between our data and the MF ground states only becomes noticeable at a small $|m|$ in the negative q_{net} region. Due to this discrepancy, we find that the pre-

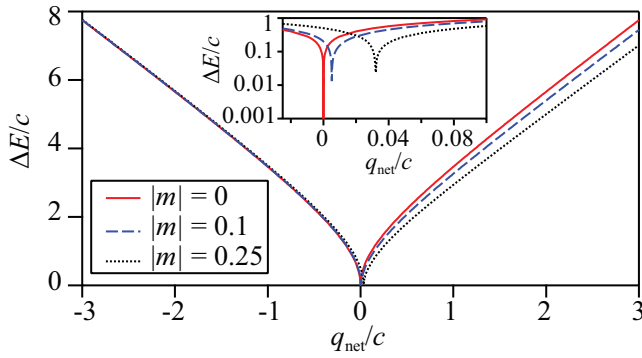


FIG. 4. (color online) The energy gap ΔE in the unit of c as a function of q_{net}/c at three $|m|$ based on Eq. 4 (see text). Inset: a magnified view of the main figure in the region of $-0.025 < q_{\text{net}}/c < 0.1$.

dicted quantum phase transition between an AFM phase and a longitudinal polar phase at $m = 0$ and $q_{\text{net}} = 0$ is replaced by a transition between a BA phase and a longitudinal polar phase. Since our experimental resolution for ρ_0 is around 0.02, Fig. 2 implies that our new method is sufficient to map out the BEC phase diagram in the positive q_{net} region at each m , and in the negative q_{net} as long as $|m| \geq 0.4$.

Figure 3 clearly summarizes the improvement provided by this new method, after comparing the theoretical MF phase diagram to an experimental phase diagram consisting of our data taken at 153 different q_{net} and m . All three predicted phases (i.e., an AFM, a polar, and a BA phases), an AFM-BA phase transition at a fixed m , and a transition between a longitudinal polar phase and a BA phase at a certain positive q_{net} are shown in the experimental phase diagram. Good agreements between our data and the MF ground states can be found everywhere in the two phase diagrams except in the region where $|m| < 0.4$ and $q_{\text{net}} < 0$. This problematic region has been marked by red solid lines in Fig. 3. Ramping microwave fields at a slower rate should help to diminish this problematic region, however, a slower rate requires holding a BEC in microwave fields for a longer time and thus inevitably leads to more atom losses and a bigger change in m . In fact, we tried quite a few different microwave ramping rates, but none of them enabled a spinor BEC to reach its MF ground states when m is very small and $q_{\text{net}} < 0$. The same problem also exists in simulation results: our simulation program cannot suggest a reasonable ramping rate to ensure an adiabatic sweep of q_{net} across a phase transition for a small m .

To understand this problem, we need to find the exact value of ΔE , the energy gap between the ground state and the first excited state in spinor BECs. Similarly to Ref. [3], we can describe a spinor BEC in the Fock space. The spin-dependent part of the Hamiltonian in a $F=1$

spinor BEC can be expressed as [3, 20, 23]

$$H = \sum_{i,j,k,l=-1}^1 \left[q_{\text{net}} k^2 a_k^\dagger a_k + \frac{c}{2} \sum_{\gamma} a_k^\dagger a_i^\dagger (F_{\gamma})_{ij} (F_{\gamma})_{kl} a_j a_l \right], \quad (4)$$

since m is conserved and there are only a finite number of atoms in a typical equilibrium state studied in this paper. Here a_k (a_k^\dagger) is the annihilation (creation) operator of the $|F=1, m_F=k\rangle$ state, and $F_{\gamma=x,y,z}$ are the spin-1 matrices. By diagonalizing the Hamiltonian in Eq. 4 and performing an exact numerical many-body calculation, we can find the energy gaps. Figure 4 shows numerical examples of ΔE at three typical $|m|$. It appears that ΔE drastically drops by more than three orders of magnitude when $|m|$ and q_{net} approach zero, as shown in the inset in Fig. 4. Therefore, it is not surprising that adiabatically sweeping q_{net} across a quantum phase transition point is not feasible at a very small m , especially at $m = 0$.

In conclusion, we have observed two types of quantum phase transitions in a spin-1 antiferromagnetic spinor BEC, and developed a new method to create the equilibrium states of spinor condensates by adiabatically sweeping a microwave field. The biggest advantage of this method is to avoid significant atom losses and detrimental changes in m at large microwave fields. We have demonstrated that this method is able to map out the phase diagram of antiferromagnetic spinor BECs for all m in the positive q_{net} region and for all negative q_{net} as long as $|m| \geq 0.4$. This method can be applied to other atomic species when applying microwave fields are required. In addition, adiabatically sweeping q_{net} across a quantum phase transition demonstrated in this paper may be a big step towards confirming other important predictions, for example, realizing massive entanglement in the vicinity of the Dicke states with spinor BECs [3].

We thank the Army Research Office, the National Science Foundation, and the Oklahoma Center for the Advancement of Science and Technology for financial support. M.W. thanks the Niblack Research Scholar program.

* yingmei.liu@okstate.edu

- [1] D. M. Stamper-Kurn and M. Ueda, Rev. Mod. Phys. **85**, 1191 (2013).
- [2] Y. Kawaguchi and M. Ueda, Phys. Rep. **520**, 253 (2012).
- [3] Z. Zhang and L.-M. Duan, Phys. Rev. Lett. **111**, 180401 (2013).
- [4] T. M. Hoang, C. S. Gerving, B. J. Land, M. Anquez, C. D. Hamley, and M. S. Chapman, Phys. Rev. Lett. **111**, 090403 (2013).
- [5] C. D. Hamley, C. S. Gerving, T. M. Hoang, E. M. Bookjans, and M. S. Chapman, Nature Physics **8**, 305 (2012).
- [6] J. Jiang, L. Zhao, M. Webb, N. Jiang, H. Yang, and Y. Liu, Phys. Rev. A **88**, 033620 (2013).

- [7] E. M. Bookjans, A. Vinit, and C. Raman, *Phys. Rev. Lett.* **107**, 195306 (2011).
- [8] A. T. Black, E. Gomez, L. D. Turner, S. Jung, and P. D. Lett, *Phys. Rev. Lett.* **99**, 070403 (2007).
- [9] Y. Liu, S. Jung, S. E. Maxwell, L. D. Turner, E. Tiesinga, and P. D. Lett, *Phys. Rev. Lett.* **102**, 125301 (2009).
- [10] Y. Liu, E. Gomez, S. E. Maxwell, L. D. Turner, E. Tiesinga, and P. D. Lett, *Phys. Rev. Lett.* **102**, 225301 (2009).
- [11] D. Jacob, L. Shao, V. Corre, T. Zibold, L. De Sarlo, E. Mimoun, J. Dalibard, and F. Gerbier, *Phys. Rev. A* **86**, 061601 (2012).
- [12] L. Zhao, J. Jiang, T. Tang, M. Webb, and Y. Liu, *Phys. Rev. A* **89**, 023608 (2014).
- [13] M.-S. Chang, Q. Qin, W. Zhang, L. You, and M. S. Chapman, *Nature Physics* **1**, 111 (2005).
- [14] A. Widera, F. Gerbier, S. Fölling, T. Gericke, O. Mandel, and I. Bloch, *New Journal of Physics* **8**, 152 (2006).
- [15] J. Kronjäger, C. Becker, P. Navez, K. Bongs, and K. Sengstock, *Phys. Rev. Lett.* **97**, 110404 (2006).
- [16] H. Schmaljohann, M. Erhard, J. Kronjäger, M. Kottke, S. van Staa, L. Cacciapuoti, J. J. Arlt, K. Bongs, and K. Sengstock, *Phys. Rev. Lett.* **92**, 040402 (2004).
- [17] T. Kuwamoto, K. Araki, T. Eno, and T. Hirano, *Phys. Rev. A* **69**, 063604 (2004).
- [18] F. Gerbier, A. Widera, S. Fölling, O. Mandel, and I. Bloch, *Phys. Rev. A* **73**, 041602(R) (2006).
- [19] S. R. Leslie, J. Guzman, M. Vengalattore, J. D. Sau, M. L. Cohen, and D. M. Stamper-Kurn, *Phys. Rev. A* **79**, 043631 (2009).
- [20] W. Zhang, D. L. Zhou, M.-S. Chang, M. S. Chapman, and L. You, *Phys. Rev. A* **72**, 013602 (2005).
- [21] Y. Kawaguchi, H. Saito, K. Kudo, and M. Ueda, *Phys. Rev. A* **82**, 043627 (2010).
- [22] A. Lamacraft, *Phys. Rev. A* **83**, 033605 (2011).
- [23] W. Zhang, S. Yi, and L. You, *New Journal of Physics* **5**, 77 (2003).